

Collision Cross-entropy and EM Algorithm for Self-labeled Classification

Zhongwen (Rex) Zhang
University of Waterloo
z889zhan@uwaterloo.ca

Yuri Boykov
University of Waterloo
yboykov@uwaterloo.ca

Abstract

We propose “collision cross-entropy” as a robust alternative to the Shannon’s cross-entropy in the context of self-labeled classification with posterior models. Assuming unlabeled data, self-labeling works by estimating latent pseudo-labels, categorical distributions y , that optimize some discriminative clustering criteria, e.g. “decisiveness” and “fairness”. All existing self-labeled losses incorporate Shannon’s cross-entropy term targeting the model prediction, softmax σ , at the estimated distribution y . In fact, σ is trained to mimic the uncertainty in y exactly. Instead, we propose the negative log-likelihood of “collision” to maximize the probability of equality between two random variables represented by distributions σ and y . We show that our loss satisfies some properties of a generalized cross-entropy. Interestingly, it agrees with the Shannon’s cross-entropy for one-hot pseudo-labels y , but the training from softer labels weakens. For example, if y is a uniform distribution at some data point, it has zero contribution to the training. Our self-labeling loss combining collision cross entropy with basic clustering criteria is convex w.r.t. pseudo-labels, but non-trivial to optimize over the probability simplex. We derive a practical EM algorithm optimizing pseudo-labels y significantly faster than generic methods, e.g. the projectile gradient descent. The collision cross-entropy consistently improves the results on multiple self-labeled clustering examples using different DNNs.

1. Introduction and Motivation

Shannon’s cross-entropy $H(y, \sigma)$ is the most common loss for training network predictions σ from ground truth labels y in the context of classification, semantic segmentation, etc. However, this loss may not be ideal for applications where the targets y are soft distributions representing various forms of uncertainty. For example, this paper is focused on self-labeled classification [16, 1, 14, 15] where the ground truth is not available and the network training

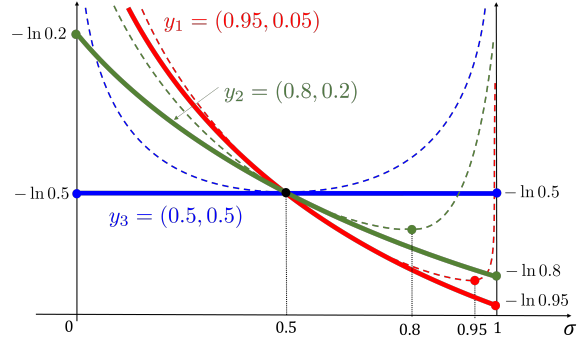


Figure 1. Collision cross-entropy $H_2(y, \sigma)$ in (9) for fixed pseudo-labels y (red, green, and blue). Assuming binary classification, all possible predictions $\sigma = (x, 1 - x) \in \Delta_2$ are represented by points $x \in [0, 1]$ on the horizontal axis. For comparison, thin dashed curves show Shannon’s cross entropy $H(y, \sigma)$ in (8). Note that H converges to infinity at both end points of the interval. In contrast, H_2 is bounded for any non-hot y . Such boundedness suggests robustness to errors in pseudo-labels y . Also, collision cross-entropy H_2 gradually turns-off the training (sets zero-gradients) as pseudo-labels become highly uncertain, see $y_3 = (0.5, 0.5)$ (solid blue). In contrast, $H(y, \sigma)$ trains the network to copy this uncertainty, e.g. observe the optimum σ for all dashed curves.

is done jointly with estimating latent pseudo-labels y . In this case soft y can represent the distribution of label uncertainty. Similar uncertainty of class labels is also natural for supervised problems where the ground truth has errors [25, 37]. In any cases of label uncertainty, if soft distribution y is used as a target in $H(y, \sigma)$, the network is trained to reproduce the uncertainty, see the dashed curves in Fig.1.

Our work is inspired by generalized entropy measures [30, 17]. Besides mathematical generality, the need for such measures “stems from practical aspects when modelling real world phenomena though entropy optimization algorithms” [27]. Similarly to L_p norms, parametric families of generalized entropy measures offer a wide spectrum of options. The Shannon’s entropy is just one of them. Other measures could be more “natural” for any given problem.

A simple experiment in Figure 2 shows that Shannon’s

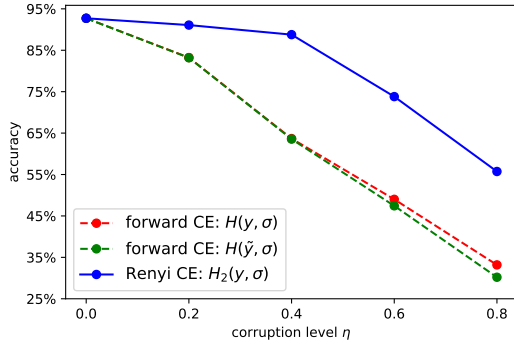


Figure 2. Robustness to label uncertainty: collision cross-entropy (9) vs Shannon’s cross-entropy (8). The test uses ResNet-18 architecture on fully-supervised image scene data with corrupted training labels. The horizontal axis shows the percentage η of training images where the correct ground truth labels was replaced by a random label. Both loss functions trained the model using soft target distributions $\hat{y} = \eta * u + (1 - \eta) * y$ representing the mixture of one-hot distribution y for the observed corrupt label and the uniform distribution u , as recommended in [25]. The vertical axis shows the test accuracy. Training with the collision cross-entropy is robust to much higher levels of label uncertainty.

cross-entropy produces deficient solutions for soft labels y compared to the proposed *collision cross-entropy*. The limitation of the standard cross-entropy is that it encourages the distributions σ and y to be equal, see the dashed curves in Fig.1. For example, the model predictions σ are trained to copy the uncertainty of the label distribution y , even when y is an uninformative uniform distribution. In contrast, our collision cross-entropy (the solid curves) gradually weakens the training as y gets less certain. This numerical property of our cross-entropy follows from its definition (9) - it maximizes the probability of “collision”, which is an event when two random variables sampled from the distributions σ and y are equal. This means that the predicted class value is equal to the latent (unobserved) label. This is significantly different from the equality of distributions $\sigma = y$ encouraged by the Shannon’s cross-entropy. For example, if y is uniform then it does not matter what the model predicts as the probability of collision $\frac{1}{K}$ would not change.

Organization of the paper: After the summary of our contributions below, Section 2 reviews the relevant background on self-labeling models/losses and generalized information measures for entropy, divergence, and cross-entropy. Then, Section 3 introduces our *collision cross entropy* measure, discusses its properties, and related formulations of Rényi cross-entropy. Section 4 formulates our self-labeling loss by replacing the Shannon’s cross entropy term in a representative state-of-the-art formulation using soft pseudo-labels [15] with our collision-cross-entropy. The obtained loss function is convex w.r.t. pseudo-labels y , which makes estimation of y amenable to generic pro-

jected gradient descent. However, Section 4 derives a much faster EM algorithm for estimating y . As common for self-labeling, optimization of the total loss w.r.t. network parameters is done via backpropagation. Section 5 presents our experiments, followed by the conclusions.

Summary of Contributions: In the context of self-labeled classification with soft pseudo-labels, we propose the *collision cross-entropy* as an alternative to the standard Shannon’s cross-entropy. The main practical advantage is its robustness to uncertainty in the labels, which could also be useful in other applications. The definition of our cross-entropy has an intuitive probabilistic interpretation that agrees with the numerical and empirical properties. Unlike the Shannon’s cross-entropy, our formulation is symmetric w.r.t. predictions σ and pseudo-labels y . This is a conceptual advantage since both σ and y are estimated/optimized distributions. Our cross-entropy allows efficient optimization of pseudo-labels by a proposed EM algorithm, that significantly accelerates a generic projected gradient descent. Our experiments show consistent improvement over multiple examples of unsupervised and weakly-supervised clustering, and several standard network architectures.

2. Background Review

We study a new generalized cross-entropy measure in the context of self-labeled classification with neural networks. The models are trained on unlabeled data, but applications with partially labeled data are also relevant. Self-labeled deep clustering is a popular area of research [4, 28]. More recently, the-state-of-the-art is achieved by discriminative clustering methods based on maximizing the mutual information between the input and the output of the deep model [3]. There is a large group of relevant methods [21, 9, 14, 16, 1, 15] and we review the most important loss functions, all of which use standard information theoretic measures such as Shannon’s entropy, cross-entropy, and KL divergence. In the second part of this section, we overview the necessary mathematical background on the generalized entropy measures, which are central to our work.

2.1. Information-based Self-labeled Clustering

The work of Bridle, Heading, and MacKay from 1991 [3] formulated *mutual information* (MI) loss for unsupervised discriminative training of neural networks using probability-type outputs, e.g. *softmax* $\sigma : \mathcal{R}^K \rightarrow \Delta^K$ mapping K logits $l_k \in \mathcal{R}$ to a point in the probability simplex Δ^K . Such output $\sigma = (\sigma_1, \dots, \sigma_K)$ is often interpreted as a *pseudo* posterior¹ over K classes, where $\sigma_k = \frac{\exp l_k}{\sum_i \exp l_i}$ is a scalar prediction for each class k .

¹“Pseudo” emphasizes that discriminative training does not lead to the true Bayesian posteriors, in general.

The unsupervised loss proposed in [3] trains the model predictions to keep as much information about the input as possible. They derived an estimate of MI as the difference between the average entropy of the output and the entropy of the average output

$$L_{mi} := -MI(c, X) \approx \overline{H(\sigma)} - H(\bar{\sigma}) \quad (1)$$

where c is a random variable representing class prediction, X represents the input, and the averaging is done over all input samples $\{X_i\}_{i=1}^M$, i.e. over M training examples. The derivation in [3] assumes that softmax represents the distribution $\Pr(c|X)$. However, since softmax is not a true posterior, the right hand side in (1) can be seen only as a *pseudo* MI loss. In any case, (1) has a clear discriminative interpretation that stands on its own: $H(\bar{\sigma})$ encourages “fair” predictions with a balanced support of all categories across the whole training data set, while $\overline{H(\sigma)}$ encourages confident or “decisive” prediction at each data point implying that decision boundaries are away from the training examples [10]. Generally, we call clustering losses for softmax models “information-based” if they use measures from the information theory, e.g. entropy.

Discriminative clustering loss (1) can be applied to deep or shallow models. For clarity, this paper distinguishes parameters w of the *representation* layers of the network computing features $f_w(X) \in \mathcal{R}^N$ for any input X and the linear classifier parameters v of the output layer computing K -logit vector $v^\top f$ for any feature $f \in \mathcal{R}^N$. The overall network model is defined as

$$\sigma(v^\top f_w(X)). \quad (2)$$

A special “shallow” case of the model in (2) is a basic linear discriminator

$$\sigma(v^\top X) \quad (3)$$

directly operating on low-level input features $f = X$. Optimization of the loss (1) for the shallow model (3) is done only over linear classifier parameters v , but the deeper network model (2) is optimized over all network parameters $[v, w]$. Typically, this is done via gradient descent or back-propagation [32, 3].

Optimization of MI losses (1) during network training is mostly done with standard gradient descent or backpropagation [3, 21, 14]. However, due to the entropy term representing the decisiveness, such loss functions are non-convex and present challenges to the gradient descent. This motivates alternative formulations and optimization approaches. For example, it is common to incorporate into the loss auxiliary variables y representing *pseudo-labels* for unlabeled data points X and to estimate them jointly with optimization of the network parameters [9, 1, 15]. Typically, such *self-labeling* approaches to unsupervised network training

iterate optimization of the loss over pseudo-labels and network parameters, similarly to the Lloyd’s algorithm for K -means [2]. While the network parameters are still optimized via gradient descent, the pseudo-labels can be optimized via more powerful algorithms.

For example, [1] formulate self-labeling using the following constrained optimization problem with discrete pseudo-labels y

$$L_{ce} = \overline{H(y, \sigma)} \quad s.t. \quad y \in \Delta_{0,1}^K \quad and \quad \bar{y} = u \quad (4)$$

where $\Delta_{0,1}^K$ are *one-hot* distributions, i.e. corners of the probability simplex Δ^K . Training of the network predictions σ is driven by the standard *cross entropy* loss $H(y, \sigma)$, which is convex assuming fixed (pseudo) labels y . With respect to variables y , the cross entropy is linear. Without the balancing constraint $\bar{y} = u$, the optimal y corresponds to the hard $\arg \max(\sigma)$. However, the balancing constraint converts this into an integer programming problem that can be approximately solved via *optimal transport* [8]. The cross-entropy in (4) encourages the network predictions σ to approximate the estimated one-hot target distributions y , which implies the decisiveness.

Self-labeling methods for unsupervised clustering can also use soft pseudo-labels $y \in \Delta^K$ as target distributions in cross-entropy $H(y, \sigma)$. In general, soft targets y are common in $H(y, \sigma)$, e.g. in the context of noisy labels [37, 35]. Softened targets y can also assist network calibration [11, 25] and improve generalization by reducing overconfidence [26]. In the context of unsupervised clustering, cross entropy $H(y, \sigma)$ with soft pseudo-labels y approximates the decisiveness since it encourages $\sigma \approx y$ implying $H(y, \sigma) \approx H(y) \approx H(\sigma)$ where the latter is the first term in (1). Instead of the hard constraint $\bar{y} = u$ used in (4), the soft fairness constraint can be represented by KL divergence $KL(\bar{y} \| u)$, as in [9, 15]. In particular, [15] formulates the following self-labeled clustering loss

$$L_{ce+kl} = \overline{H(y, \sigma)} + KL(\bar{y} \| u) \quad (5)$$

encouraging the decisiveness and fairness as discussed. Similarly to (4), the network parameters in loss (5) are trained by the standard cross-entropy term, but optimization over relaxed pseudo-labels $y \in \Delta^K$ is relatively easy due to convexity. While there is no closed form solution, the authors offer an efficient approximate solver for y . Iterating steps that estimate pseudo-labels y and optimize the model parameters resembles the Lloyd’s algorithm for K-means. The results in [15] also establish a formal relation between the loss (5) and the K -means objective.

2.2. Generalized Entropy Measures

Below, we review relevant generalized formulations of the information theoretic concepts: entropy, divergence,

and cross-entropy. Rényi [30] introduced the *entropy of order* $\alpha > 0$ for any probability distribution p

$$H_\alpha(p) := \frac{1}{1-\alpha} \ln \sum_k p_k^\alpha \quad (\alpha \neq 1)$$

derived as the most general measure of uncertainty in p satisfying four intuitively evident postulates. The entropy measures the average information and the order parameter α relates to the power of the corresponding mean statistic [40]. The general formula above includes the Shannon's entropy

$$H(p) = - \sum_k p_k \ln p_k$$

as a special case when $\alpha \rightarrow 1$. The quadratic or second-order Rényi entropy

$$H_2(p) := - \ln \sum_k p_k^2 \quad (6)$$

is also known as a *collision entropy* since it is a negative log-likelihood of a “collision” or “rolling double” when two i.i.d. samples from distribution p have equal values.

Basic characterization postulates in [30] also lead to the general Rényi formulation of the *divergence*, also known as the *relative entropy*, of order $\alpha > 0$

$$D_\alpha(p \mid q) := \frac{1}{\alpha-1} \ln \sum_k p_k^\alpha q_k^{1-\alpha} \quad (\alpha \neq 1)$$

defined for any pair of distributions p and q . This reduces to the standard KL divergence when $\alpha \rightarrow 1$

$$D(p, q) = \sum_k p_k \ln \frac{p_k}{q_k} \quad (7)$$

and to the *Bhattacharyya distance* for $\alpha = \frac{1}{2}$.

Optimization of entropy and divergence [23] is fundamental to many machine learning problems [34, 19, 18, 27], including pattern classification and cluster analysis [33]. However, the entropy-related terminology is often mixed-up. For example, when discussing the *cross-entropy minimization principle* (MinxEnt), many of the references cited earlier in this paragraph define *cross-entropy* using the expression for KL-divergence (7). Nowadays, it is standard to define the Shannon's cross-entropy as

$$H(p, q) = - \sum_k p_k \ln q_k. \quad (8)$$

One simple explanation for the confusion is that KL-divergence $D(p, q)$ and cross-entropy $H(p, q)$ as functions of q only differ by a constant if p is a fixed known target, which is often the case.

3. Collision Cross-Entropy

Minimizing divergence enforces proximity between two distributions, which may work as a loss for training model predictions σ with labels y , for example if y are ground truth one-hot labels. However, if y are pseudo-labels that are estimated jointly with σ , proximity between y and σ is not a good criteria for the loss. For example, highly uncertain model predictions σ in combination with uniformly distributed pseudo-labels y correspond to the optimal zero divergence, but this is not a very useful result for self-labeling. Instead, all existing self-labeling losses for deep clustering minimize Shannon's cross-entropy (8) that reduces the divergence and uncertainty at the same time

$$H(y, \sigma) \equiv D(y, \sigma) + H(y).$$

The entropy term corresponds to the “decisiveness” constraint in unsupervised discriminative clustering [3, 16, 1, 14, 15]. In general, it is recommended as a regularizer for unsupervised and weakly-supervised network training [10] to encourage decision boundaries away from the data points implicitly increasing the decision margins.

We propose a new form of cross-entropy

$$H_2(p, q) := - \ln \sum_k p_k q_k \quad (9)$$

that we call *collision cross-entropy* since it extends the collision entropy in (6). Indeed, (9) is the negative log-probability of an event that two random variables with (different) distributions p and q are equal. When training softmax σ with pseudo-label distribution y , the collision event is the exact equality of the predicted class and the pseudo-label, where these are interpreted as specific outcomes for random variables with distributions σ and y . Note that the collision event, i.e. the equality of two random variables, has very little to do with the equality of distributions $\sigma = y$. The collision may happen when $\sigma \neq y$, as long as $\sigma \cdot y > 0$. Vice versa, this event is not guaranteed even when $\sigma = y$. It will happen *almost surely* only if the two distributions are the same one-hot. However, if the distributions are both uniform, the collision probability is only $1/K$.

As easy to check, the collision cross-entropy (9) can be equivalently represented as

$$H_2(p, q) \equiv - \ln \cos(p, q) + \frac{H_2(p) + H_2(q)}{2}$$

where $\cos(p, q)$ is the cosine of the angle between p and q as vectors in \mathcal{R}^K and H_2 is the collision entropy (6). At least informally, the first term corresponds to a “distance” between the two distributions: it is non-negative, equals 0 iff $p = q$, and $-\ln \cos(\cdot)$ is a convex function of an angle, which can be interpreted as a spherical metric. Thus, analogously to the Shannon's cross entropy, H_2 is the sum of divergence and entropy.

Formula (9) can be found as a definition of quadratic Rényi cross-entropy [27, 29, 41]. However, we could not identify information-theoretic axioms characterizing a generalized cross-entropy. Rényi himself did not discuss the concept of cross-entropy in his seminal work [30]. Also, two different formulations of “natural” and “shifted” Rényi cross-entropy of arbitrary order could be found in [40, 38]. In particular, the shifted version of order 2 agrees with our formulation of collision cross-entropy (9). However, lack of the postulates or characterization for the cross-entropy, and existence of multiple non-equivalent formulations did not give us confidence to use the name Rényi. Instead, we use “collision” due to its clear intuitive interpretation of the loss (9). But, the term “cross-entropy” is used only informally.

The numerical and empirical properties of the collision cross-entropy (9) are sufficiently different from the Shannons cross-entropy (8). Figure 1 illustrates $H_2(y, \sigma)$ as a function of σ for different label distributions y . For confident y it behaves the same way as the standard cross entropy $H(y, \sigma)$, but softer low-confident labels y naturally have little influence on the training. In contrast, the standard cross entropy encourages prediction σ to be the exact copy of uncertainty in distribution y . Standard self-labeling methods based on $H(y, \sigma)$ often “prune out” uncertain pseudo-labels [5]. Collision cross entropy $H_2(y, \sigma)$ makes such heuristics redundant. We also demonstrate this “robustness to label uncertainty” on an example where the ground truth labels are corrupted by different level of noise, see Fig.2. This artificial fully-supervised test is used only to compare the robustness of (9) and (8) in complete isolation from other terms in the self-labeled clustering losses, which are at the focus in this work.

Due to the symmetry of the arguments in (9), such robustness of $H_2(y, \sigma)$ also works the other way around. Indeed, self-labeling losses are often used for both training σ and estimating y : the loss is iteratively optimized over predictions σ (i.e. model parameters responsible for it) and over pseudo-label distribution y . Thus, it helps if y also demonstrates “robustness to prediction uncertainty”.

4. Our Self-labeling Loss and EM

Based on prior work (5), we replace the standard cross-entropy by our collision cross-entropy to formulate our self-labeling loss as follows:

$$L_{CCE} := \overline{H_2(y, \sigma)} + \lambda KL(\bar{y} \| u) \quad (10)$$

To optimize such loss, we iterate between two alternating steps for σ and y . For σ , we use the standard stochastic gradient descent algorithms[31]. For y , we use the projected gradient descent (PGD) [6]. However, the speed of PGD is slow as shown in Table 1 especially when there are more classes. This motivates us to find more efficient algorithms

for optimizing y . To derive such algorithm, we made a minor change to (18) by switching the order of variables in the divergence term:

$$L_{CCE+} := \overline{H_2(y, \sigma)} + \lambda KL(u \| \bar{y}) \quad (11)$$

Such change allows us to use the Jensen’s inequality on the divergence term to derive an efficient EM algorithm while the quality of the self-labeled classification results are almost the same as shown in the supplementary material.

	running time in sec. per iteration			number of iterations (to convergence)			running time in sec. (to convergence)		
	K_2	K_{20}	K_{200}	K_2	K_{20}	K_{200}	K_2	K_{20}	K_{200}
PGD (η_1)	7.8e-4	2.9e-3	6.7e-2	326	742	540	0.25	2.20	36.25
PGD (η_2)	9.3e-4	3.3e-3	6.8e-2	101	468	344	0.09	1.55	23.35
PGD (η_3)	9.9e-4	3.2e-3	7.0e-2	24	202	180	0.02	0.65	12.60
EM	1.8e-3	1.6e-3	5.1e-3	25	53	71	0.04	0.09	0.36

Table 1. Comparison of our EM algorithm to Projected Gradient Descent (PGD). K_2 , K_{20} and K_{200} stand for the number of classes. η is the step size. For K_2 , $\eta_1 \sim \eta_3$ are 1, 10 and 20 respectively. For K_{20} and K_{200} , $\eta_1 \sim \eta_3$ are 0.1, 1 and 5 respectively. Higher step size may lead to the divergence of the PGD.

EM algorithm for optimizing y We derive the EM algorithm introducing latent variables, K distributions $S^k \in \Delta^M$ representing normalized support for each cluster over M data points. We refer to each vector S^k as a *normalized cluster* k . Note the difference with distributions represented by pseudo-labels $y \in \Delta^K$ showing support for each class at a given data point. Since we explicitly use individual data points below, we will start to carefully index them by $i \in \{1, \dots, M\}$. Thus, we will use $y_i \in \Delta^K$ and $\sigma_i \in \Delta^K$. Individual components of distribution $S^k \in \Delta^M$ corresponding to data point i will be denoted by scalar S_i^k .

First, we expand (19) introducing the latent variables $S^k \in \Delta^M$

$$L_{CCE+} \stackrel{c}{=} \overline{H_2(y, \sigma)} + \lambda H(u, \bar{y}) \quad (12)$$

$$= \overline{H_2(y, \sigma)} - \lambda \sum_k u^k \ln \sum_i S_i^k \frac{y_i^k}{S_i^k M}$$

$$\leq \overline{H_2(y, \sigma)} - \lambda \sum_k \sum_i u^k S_i^k \ln \frac{y_i^k}{S_i^k M} \quad (13)$$

Due to the convexity of negative log, we apply the Jensen’s inequality to derive an upper bound, i.e. (13), to L_{CCE+} . Such bound becomes tight when:

$$\mathbf{E step : } S_i^k = \frac{y_i^k}{\sum_j y_j^k} \quad (14)$$

Next, we derive the M step. Introducing the hidden variable S breaks the fairness term into the sum of independent terms for pseudo-labels $y_i \in \Delta_K$ at each data point i . The solution for S does not change (E step). Lets focus on the

loss with respect to y . The collision cross-entropy (CCE) also breaks into the sum of independent parts for each y_i . For simplicity, we will drop all indices i in variables y_i^k , S_i^k , σ_i^k . Then, the combination of CCE loss with the corresponding part of the fairness constraint can be written for each $y = \{y_k\} \in \Delta_K$ as

$$-\ln \sum_k \sigma_k y_k - \lambda \sum_k u_k S_k \ln y_k. \quad (15)$$

First, observe that this loss must achieve its global optimum in the interior of the simplex if $S_k > 0$ and $u_k > 0$ for all k . Indeed, the second term enforces the “log-barrier” at the boundary of the simplex. Thus, we do not need to worry about KKT conditions in this case. Note that S_k might be zero, in which case we need to consider the full KKT conditions. However, the Property 1 that will be mentioned later eliminates such concern if we use positive initialization. For completeness, we also give the detailed derivation for such case and it can be found in the supplementary material.

Adding the Lagrange multiplier γ for the simplex constraint, we get an unconstrained loss

$$-\ln \sum_k \sigma_k y_k - \lambda \sum_k u_k S_k \ln y_k + \gamma \left(\sum_k y_k - 1 \right)$$

that must have a stationary point inside the simplex.

Computing partial derivatives w.r.t. y_k , we get the following stationary point equation for each k

$$\gamma y_k = \frac{\sigma_k y_k}{\sigma^\top y} + \lambda u_k S_k.$$

Summing these for all k , we have

$$\gamma = 1 + \lambda u^\top S.$$

Now we get the following equation for y

$$y_k \left(1 + \lambda u^\top S - \frac{\sigma_k}{\sigma^\top y} \right) = \lambda u_k S_k$$

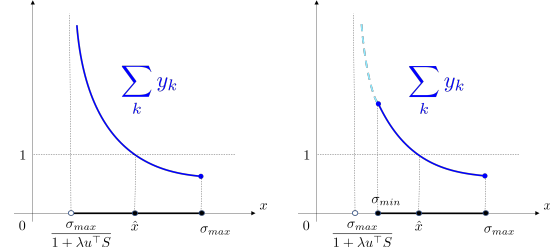
This equation is necessarily solved by pseudo-labels $y = \{y_k\} \in \Delta_K$ such that

$$y_k = \frac{\lambda u_k S_k}{\lambda u^\top S + 1 - \frac{\sigma_k}{x}} \quad \text{for some } x \in \left(\frac{\sigma_{max}}{1 + \lambda u^\top S}, \sigma_{max} \right] \quad (16)$$

where σ_{max} is the largest σ_k . The specified interval domain for x is necessary for the solution.

Theorem 1. [M-step solution]: *The sum $\sum_k y_k$ as in (16) is positive, continuous, convex, and monotonically decreasing function of x on the specified interval, see Fig.3(a). Moreover, there exists a unique solution $\{y_k\} \in \Delta_K$ and x such that*

$$\sum_k y_k \equiv \sum_k \frac{\lambda u_k S_k}{\lambda u^\top S + 1 - \frac{\sigma_k}{x}} = 1 \quad \text{and} \quad x \in \left(\frac{\sigma_{max}}{1 + \lambda u^\top S}, \sigma_{max} \right] \quad (17)$$



(a) general case

(b) special case when

$$\sigma_{min} > \frac{\sigma_{max}}{1 + \lambda u^\top S}$$

Figure 3. Collision Cross Entropy - M step (20): the sum $\sum_k y_k$ is a positive, continuous, convex, and monotonically decreasing function of x on the specified interval (a). In case $\sigma_{min} > \frac{\sigma_{max}}{1 + \lambda u^\top S}$ (b), one can further restrict the search interval for x . The fact that $\sum_k y_k \geq 1$ for $x = \sigma_{min}$ follows from an argument similar to the one below (16) showing that $\sum_k y_k \leq 1$ for $x = \sigma_{max}$.

Proof. All y_k in (16) are positive, continuous, convex, and monotonically decreasing functions of x on the specified interval. Thus, $\sum y_k$ behaves similarly. Assuming that max is the index of prediction σ_{max} , we have $y_{max} \rightarrow +\infty$ when approaching the interval’s left endpoint $x \rightarrow \frac{\sigma_{max}}{1 + \lambda u^\top S}$. Thus, $\sum y_k > 1$ for smaller values of x . At the right endpoint $x = \sigma_{max}$ we have $y_k \leq \frac{\lambda u_k S_k}{\lambda u^\top S}$ for all k implying $\sum y_k \leq 1$. Monotonicity and continuity of $\sum y_k$ w.r.t. x imply the theorem. \square

The monotonicity and convexity of $\sum_k y_k$ with respect to x suggest that the problem (20) formulated in Theorem 2 allows efficient algorithms for finding the corresponding unique solution. For example, one can use the iterative Newton’s updates searching for x in the specified interval. The following Lemma gives us a proper start point for Newton’s method.

Lemma 1. *Assuming $u_k S_k$ is positive for each k , then the reachable left end point in Theorem 2 can be written as*

$$l := \max_k \frac{\sigma_k}{1 + \lambda u^\top S - \lambda u_k S_k}.$$

Proof is provided in the supplementary material. Next, we give the property about the positivity of the solution. This property implies that if our EM algorithm has only (strictly) positive variables S_k or y_k at initialization, these variables will remain positive during all iterations.

Property 1. *For any category k such that $u_k > 0$, the set of strictly positive variables y_k or S_k can only grow during iterations of our EM algorithm for the loss (21) based on the Rényi cross-entropy.*

Proof. As obvious from the E-step (14), it is sufficient to prove this for variables y_k . If $y_k = 0$, then the E-step (14)

gives $S_k = 0$. According to the M-step for the case of Rényi cross-entropy, variable y_k may become (strictly) positive at the next iteration if $\sigma_k = \sigma_{max}$. Once y_k becomes positive, the following E-step (14) produces $S_k > 0$. Then, the fairness term effectively enforces the log-barrier from the corresponding simplex boundary making M-step solution $y_k = 0$ prohibitively expensive. Thus, y_k will remain strictly positive at all later iterations. \square

Note that Property 1 does not rule out the possibility that y_k may become arbitrarily close to zero during EM iterations. Empirically, we did not observe any numerical issues.

Besides, some properties of our loss function using collision cross-entropy are illustrated by the following simple examples where a closed-form solution for y can be derived.

Example 1. When $\lambda \rightarrow \infty$ and the loss (21) is focused on the fairness term, equation (20) has an obvious closed-form solution

$$y_k = \frac{u_k S_k}{u^\top S}$$

obtained for any x in the specified interval.

Example 2. When $\lambda = 0$ the loss (21) if focused on collision cross-entropy and the corresponding solution is a *one-hot* distribution

$$y = \mathbf{1}_{max}$$

where $max = \arg \max_k \sigma_k$ is the index in σ_{max} . Equation (20) converges to this solution for

$$x = \frac{\sigma_{max}}{1 + \lambda(u^\top S - u_{max} S_{max})} \xrightarrow{\lambda \rightarrow 0} \sigma_{max}.$$

The corresponding solutions y in (16) converge to a “corner” of the simplex as $\lambda \rightarrow 0$. However, for any strictly-positive $\lambda > 0$, the solution y is in the interior of the simplex assuming all S_k and u_k are non-zero.

Example 3. Consider the case where $\sigma = \mathbf{1}_c$ for any given category c . It is easy to check that

$$y_k = \frac{1_{[k=c]} + \lambda u_k S_k}{1 + \lambda u^\top S}$$

where $\sigma_k \equiv 1_{[k=c]}$ are the binary components of the *one-hot* distribution $\sigma = \mathbf{1}_c$.

The complete algorithm is give in Algorithm 1. Inspired by [36, 14], we also update our y in each batch and empirically this improves our results. Intuitively, updating y on the fly can prevent the network from being easily trapped in some local minima created by the incorrect pseudo-labels.

Algorithm 1: Optimization for (19)

```

Input : network parameters and dataset
Output: network parameters
for each epoch do
  for each iteration do
    Initialize  $y$  by the network output at current
    stage as a warm start;
    while not convergent do
       $S_i^k = \frac{y_i^k}{\sum_j y_j^k}$ ;
      find  $y_i^k$  using Newton's method;
    end
    Update network using loss  $\overline{H_2}(y, \sigma)$  via
    stochastic gradient descent
  end
end

```

5. Experiments

We apply our new loss to self-labeled classification problems in both shallow and deep settings, as well as weakly-supervised modes. Our approach achieves either the best or highly competitive results across all the datasets and is therefore more robust. The details on the architecture and training will be found in the supplementary material.

Dataset For self-labeled classification problems, we use four standard datasets: MNIST [24], CIFAR10/100 [39] and STL10 [7]. The training and test data are the same. As for weakly-supervised setting, we conduct experiments on CIFAR10 and STL10. We split the data into training and test sets as suggested by [16].

Evaluation As for the evaluation on self-labeled classification, we set the number of clusters to the number of ground-truth categories and we adopt the standard method [22] by finding the best one-to-one mapping between clusters and labels. We use the accuracy as the measure for both self-labeled and weakly-supervised settings while the latter calculates the accuracy on the test set.

5.1. Low-level Self-labeled Classification

In this section, we test our loss as a proper clustering loss and compare it to the widely used Kmeans (generative) and other related losses (discriminative). “Low-level” here means that the features are fixed and we use the pretrained Resnet-50 [13] to extract the features. We use standard sklearn package to implement Kmeans. We use one-layer linear classifier followed by softmax for all other losses including our loss. We report the average accuracy and standard deviation over 6 randomly initialized trials in Table 5. Note that MI-GD [3, 21] has no pseudo-labels in the loss

formula and the authors directly use the gradient descent to optimize the classifier parameters. We also juxtapose it here because it is the most basic discriminative method for clustering.

	STL10	CIFAR10	CIFAR100-20	MNIST
Kmeans	85.20%(5.9)	67.78%(4.6)	42.99%(1.3)	47.62%(2.1)
MI-GD [3, 21]	89.56%(6.4)	72.32%(5.8)	43.59%(1.1)	52.92%(3.0)
MI-ADM [15]	88.64%(7.1)	60.57%(3.3)	41.22%(1.4)	50.61%(1.3)
SeLa [1]	90.33%(4.8)	63.31%(3.7)	40.74%(1.1)	52.38%(5.2)
Our	92.33%(6.4)	73.51%(6.3)	43.72%(1.1)	58.4%(3.2)

Table 2. Comparison of different methods on clustering with fixed features extracted from Resnet-50. The numbers are the average accuracy and the standard deviation over trials. We only use the 20 coarse categories for CIFAR100.

5.2. Deep Self-labeled Classification

For deep setting, we also train the features simultaneously while doing the clustering. We do not include Kmeans here since Kmeans is a generative method, which essentially estimates the distribution of the underlying data, and is not well-defined when the data/feature is not fixed.

We also adopted self-augmentation techniques, following [14, 16, 1]. Such technique is important for enforcing neural networks to learn augmentation-invariant features, which are often semantically meaningful. While [16] designed their loss directly based on such technique, our loss and [21, 1, 15] are more general for clustering without any guarantee to generate semantic clusters. Thus, for fair comparison and more reasonable results, we combine such augmentation technique into network training. Specifically, we achieved this by setting $\sigma_i = \mathbb{E}_t[\sigma(t(X_i))]$. For each image, we generate two augmentations sampled from “horizontal flip”, “rotation” and “color distortion”.

	STL10	CIFAR10	CIFAR100-20	MNIST
MI-D [14]	25.28%(0.5)	21.4%(0.5)	14.39%(0.7)	92.90%(6.3)
IIC [16]	24.12%(1.7)	21.3%(1.4)	12.58%(0.6)	82.51%(2.3)
SeLa [1]	23.99%(0.9)	24.16%(1.5)	15.34%(0.3)	52.86%(1.9)
MI-ADM [15]	23.37%(0.9)	23.26%(0.6)	14.02%(0.5)	78.88%(3.3)
Our	25.98%(1.1)	24.26%(0.8)	15.14%(0.5)	95.11%(4.3)

Table 3. Quantitative comparison of self-labeled classification methods with simultaneous feature training from the scratch. The network architecture is VGG-4. We reuse the code published by [16, 1, 14] and use our improved implementation of [15] (also for Table 5).

Note that the numbers are not as high as reported in the prior work because we are using a relatively simple network architecture and using self-augmentation as the only additional training technique/trick. We keep the experimental settings as simple as possible and focus on the fair comparison among different loss functions along with their own op-

timization algorithms. Changing to more complex architectures while training from the scratch may need more techniques, such as auxiliary over-clustering and multiple sub-heads [16], other than the self-augmentation to learn reasonable features for clustering. Our Table 5 can also give us a glimpse of how different losses work using a more complex network architecture for feature generation even though features are fixed in that scenario.

5.3. Weakly-supervised Classification

Although our paper is focused on the self-labeled classification, we find it also interesting and natural to test our loss under weakly-supervised setting where partial data is provided with ground-truth labels. We use the standard cross-entropy loss for labeled data and directly add it to the self-labeled loss to train the network from the scratch.

	0.1		0.05		0.01	
	STL10	CIFAR10	STL10	CIFAR10	STL10	CIFAR10
Only seeds	40.27%	58.77%	36.26%	54.27%	26.1%	39.01%
+ MI-D [14]	47.39%	65.54%	40.73%	61.4%	26.54%	46.97%
+ IIC [16]	44.73%	66.5%	33.6%	61.17%	26.17%	47.21%
+ SeLa [1]	44.84%	61.5%	36.4%	58.35%	25.08%	47.19%
+ MI-ADM [15]	45.83%	62.51%	40.41%	57.05%	25.79%	45.91%
+ Our	47.79%	66.17%	41.71%	61.59%	27.18%	47.22%

Table 4. Quantitative results for weakly-supervised classification on STL10 and CIFAR10. The network architecture is VGG-4. The numbers 0.1, 0.05 and 0.01 correspond to different ratio of labels used for supervision. “Only seeds” means we only use standard cross-entropy loss on labelled data for training.

6. Conclusion

We propose a new collision cross-entropy loss for self-labeled classification. Such loss is naturally interpreted as measuring the probability of the equality between two random variables represented by the two distributions σ and y , which perfectly fits the goal of self-labeled classification. It is symmetric w.r.t. the two distributions instead of treating one as the target, like the standard cross-entropy. While the latter makes the network copy the uncertainty in estimated pseudo-labels, our cross-entropy naturally weakens the training on data points where pseudo labels are more uncertain. This makes our cross-entropy robust to labeling errors. In fact, the robustness works both for prediction and for pseudo-labels due to the symmetry. We also developed an efficient EM algorithm for optimizing the pseudo-labels. Such EM algorithm converges faster and takes much less time compared to the standard projected gradient descent, especially when there are more classes. Experimental results show that our method consistently produces top or near-top results on all tested self-labeled and weakly-supervised benchmarks.

References

- [1] Yuki Markus Asano, Christian Rupprecht, and Andrea Vedaldi. Self-labelling via simultaneous clustering and representation learning. In *International Conference on Learning Representations*, 2020. [1](#), [2](#), [3](#), [4](#), [8](#)
- [2] Christopher M. Bishop. *Pattern Recognition and Machine Learning*. Springer, 2006. [3](#)
- [3] John S. Bridle, Anthony J. R. Heading, and David J. C. MacKay. Unsupervised classifiers, mutual information and 'phantom targets'. In *NIPS*, pages 1096–1101, 1991. [2](#), [3](#), [4](#), [7](#), [8](#)
- [4] Jianlong Chang, Lingfeng Wang, Gaofeng Meng, Shiming Xiang, and Chunhong Pan. Deep adaptive image clustering. In *Proceedings of the IEEE international conference on computer vision*, pages 5879–5887, 2017. [2](#)
- [5] Jianlong Chang, Lingfeng Wang, Gaofeng Meng, Shiming Xiang, and Chunhong Pan. Deep adaptive image clustering. In *International Conference on Computer Vision (ICCV)*, pages 5879–5887, 2017. [5](#)
- [6] Yunmei Chen and Xiaojing Ye. Projection onto a simplex, 2011. [5](#)
- [7] Adam Coates, Andrew Ng, and Honglak Lee. An analysis of single-layer networks in unsupervised feature learning. In *Proceedings of the fourteenth international conference on artificial intelligence and statistics*, pages 215–223. JMLR Workshop and Conference Proceedings, 2011. [7](#), [12](#)
- [8] Marco Cuturi. Sinkhorn distances: Lightspeed computation of optimal transport. *Advances in neural information processing systems*, 26, 2013. [3](#)
- [9] Kamran Ghasedi Dizaji, Amirhossein Herandi, Cheng Deng, Weidong Cai, and Heng Huang. Deep clustering via joint convolutional autoencoder embedding and relative entropy minimization. In *Proceedings of the IEEE international conference on computer vision*, pages 5736–5745, 2017. [2](#), [3](#)
- [10] Yves Grandvalet and Yoshua Bengio. Semi-supervised learning by entropy minimization. *Advances in neural information processing systems*, 17, 2004. [3](#), [4](#)
- [11] Chuan Guo, Geoff Pleiss, Yu Sun, and Kilian Q Weinberger. On calibration of modern neural networks. In *International conference on machine learning*, pages 1321–1330. PMLR, 2017. [3](#)
- [12] Kaiming He, Xiangyu Zhang, Shaoqing Ren, and Jian Sun. Delving deep into rectifiers: Surpassing human-level performance on imagenet classification. In *Proceedings of the IEEE international conference on computer vision*, pages 1026–1034, 2015. [12](#)
- [13] Kaiming He, Xiangyu Zhang, Shaoqing Ren, and Jian Sun. Deep residual learning for image recognition. In *Proceedings of the IEEE conference on computer vision and pattern recognition*, pages 770–778, 2016. [7](#)
- [14] Weihua Hu, Takeru Miyato, Seiya Tokui, Eiichi Matsumoto, and Masashi Sugiyama. Learning discrete representations via information maximizing self-augmented training. In *International conference on machine learning*, pages 1558–1567. PMLR, 2017. [1](#), [2](#), [3](#), [4](#), [7](#), [8](#)
- [15] Mohammed Jabi, Marco Pedersoli, Amar Mitiche, and Ismail Ben Ayed. Deep clustering: On the link between discriminative models and k-means. *IEEE Transactions on Pattern Analysis and Machine Intelligence*, 43(6):1887–1896, 2021. [1](#), [2](#), [3](#), [4](#), [8](#)
- [16] Xu Ji, Joao F Henriques, and Andrea Vedaldi. Invariant information clustering for unsupervised image classification and segmentation. In *Proceedings of the IEEE/CVF International Conference on Computer Vision*, pages 9865–9874, 2019. [1](#), [2](#), [4](#), [7](#), [8](#), [12](#)
- [17] Jagat N. Kapur. *Measures of Information and Their Applications*. John Wiley and Sons, 1994. [1](#)
- [18] Jagat N. Kapur and Hiremagalur K. Kesavan. *Entropy Optimization Principles and Applications*. Springer, 1992. [4](#)
- [19] Hiremagalur K. Kesavan and Jagat N. Kapur. *Maximum Entropy and Minimum Cross-Entropy Principles: Need for a Broader Perspective*, pages 419–432. Springer, 1990. [4](#)
- [20] Diederik P Kingma and Jimmy Ba. Adam: A method for stochastic optimization. In *ICLR (Poster)*, 2015. [12](#)
- [21] Andreas Krause, Pietro Perona, and Ryan Gomes. Discriminative clustering by regularized information maximization. *Advances in neural information processing systems*, 23, 2010. [2](#), [3](#), [7](#), [8](#)
- [22] Harold W Kuhn. The hungarian method for the assignment problem. *Naval research logistics quarterly*, 2(1-2):83–97, 1955. [7](#)
- [23] Solomon Kullback. *Information Theory and Statistics*. Wiley, New York, 1959. [4](#)
- [24] Y. Lecun, L. Bottou, Y. Bengio, and P. Haffner. Gradient-based learning applied to document recognition. *Proceedings of the IEEE*, 86(11):2278–2324, 1998. [7](#), [12](#)
- [25] Rafael Müller, Simon Kornblith, and Geoffrey E Hinton. When does label smoothing help? *Advances in neural information processing systems*, 32, 2019. [1](#), [2](#), [3](#)
- [26] Gabriel Pereyra, George Tucker, Jan Chorowski, Lukasz Kaiser, and Geoffrey Hinton. Regularizing neural networks by penalizing confident output distributions. 2017. [3](#)
- [27] Jose C. Principe, Dongxin Xu, and John W. Fisher III. Information-theoretic learning. *Advances in unsupervised adaptive filtering*, 3 2000. [1](#), [4](#), [5](#)
- [28] Alec Radford, Luke Metz, and Soumith Chintala. Unsupervised representation learning with deep convolutional generative adversarial networks. *arXiv preprint arXiv:1511.06434*, 2015. [2](#)
- [29] Sudhir Rao, Allan de Medeiros Martins, and José C. Príncipe. Mean shift: An information theoretic perspective. *Pattern Recognition Letters*, 30:222–230, February 2009. [5](#)
- [30] Alfréd Rényi. On measures of entropy and information. *Fourth Berkeley Symp. Math. Stat. Probab.*, 1:547–561, 1961. [1](#), [4](#), [5](#)
- [31] Sebastian Ruder. An overview of gradient descent optimization algorithms. *arXiv preprint arXiv:1609.04747*, 2016. [5](#)
- [32] David E Rumelhart, Geoffrey E Hinton, and Ronald J Williams. Learning representations by back-propagating errors. *Nature*, 323(6088):533–536, 1986. [3](#)
- [33] John E. Shore and Robert M. Gray. Minimum cross-entropy pattern classification and cluster analysis. *IEEE Transactions on Pattern Analysis and Machine Intelligence*, pages 11–17, January 1982. [4](#)

- [34] John E. Shore and Rodney W. Johnson. Axiomatic derivation of the principle of maximum entropy and the principle of minimum cross-entropy. *IEEE Transactions on Information Theory*, 26(1):547–561, January 1980. [4](#)
- [35] Hwanjun Song, Minseok Kim, Dongmin Park, Yooju Shin, and Jae-Gil Lee. Learning from noisy labels with deep neural networks: A survey. *IEEE Transactions on Neural Networks and Learning Systems*, 2022. [3](#)
- [36] Jost Tobias Springenberg. Unsupervised and semi-supervised learning with categorical generative adversarial networks. In *International Conference on Learning Representations*, 2015. [7](#)
- [37] Daiki Tanaka, Daiki Ikami, Toshihiko Yamasaki, and Kiyoharu Aizawa. Joint optimization framework for learning with noisy labels. In *Proceedings of the IEEE conference on computer vision and pattern recognition*, pages 5552–5560, 2018. [1, 3](#)
- [38] Ferenc C. Thierrin, Fady Alajaji, and Tamás Linder. Rényi cross-entropy measures for common distributions and processes with memory. *Entropy*, 24(10), October 2022. [5](#)
- [39] Antonio Torralba, Rob Fergus, and William T Freeman. 80 million tiny images: A large data set for nonparametric object and scene recognition. *IEEE transactions on pattern analysis and machine intelligence*, 30(11):1958–1970, 2008. [7, 12](#)
- [40] Francisco J. Valverde-Albacete and Carmen Peláez-Moreno. The case for shifting the Rényi entropy. *Entropy*, 21(1), January 2019. [4, 5](#)
- [41] Xiao-Tong Yuan and Bao-Gang Hu. Robust feature extraction via information theoretic learning. In *International Conference on Machine Learning, (ICML)*, page 1193–1200, June 2009. [5](#)

A. Self-supervision Loss Comparison

$$L_{CCE} := \overline{H_2(y, \sigma)} + \lambda KL(\bar{y} \| u) \quad (18)$$

$$L_{CCE+} := \overline{H_2(y, \sigma)} + \lambda KL(u \| \bar{y}) \quad (19)$$

	STL10	CIFAR10	CIFAR100-20	MNIST
(1)	92.32%(6.3)	73.51%(6.4)	43.73%(1.1)	58.4%(3.2)
(2)	92.33%(6.4)	73.51%(6.3)	43.72%(1.1)	58.4%(3.2)

Table 5. Using fixed features extracted from Resnet-50. The numbers are the average accuracy and standard deviation over trials.

	STL10	CIFAR10	CIFAR100-20	MNIST
(1)	25.98%(1.0)	24.26%(0.8)	15.13%(0.6)	95.10%(4.2)
(2)	25.98%(1.1)	24.26%(0.8)	15.14%(0.5)	95.11%(4.3)

Table 6. With simultaneous feature training from the scratch. The network architecture is VGG-4.

B. Proof for Lemma 1

Theorem 2. [M-step solution]: *The sum $\sum_k y_k$ as below is positive, continuous, convex, and monotonically decreasing function of x on the specified interval. Moreover, there exists a unique solution $\{y_k\} \in \Delta_k$ and x such that*

$$\sum_k y_k \equiv \sum_k \frac{\lambda u_k S_k}{\lambda u^\top S + 1 - \frac{\sigma_k}{\lambda u^\top S}} = 1 \quad \text{and} \quad x \in \left(\frac{\sigma_{max}}{1 + \lambda u^\top S}, \sigma_{max} \right] \quad (20)$$

Lemma 2. *Assuming $u_k S_k$ is positive for each k , then the reachable left end point in Theorem 2 can be written as*

$$l := \max_k \frac{\sigma_k}{1 + \lambda u^\top S - \lambda u_k S_k}.$$

Proof. Firstly, we prove that l is (strictly) inside the interior of the interval in Theorem 2. For the left end point, we have

$$\begin{aligned} l &:= \max_k \frac{\sigma_k}{1 + \lambda u^\top S - \lambda u_k S_k} \\ &\geq \frac{\sigma_{max}}{1 + \lambda u^\top S - \lambda u_{max} S_{max}} \\ &> \frac{\sigma_{max}}{1 + \lambda u^\top S} \quad u_{max} S_{max} \text{ is positive} \end{aligned}$$

For the right end point, we have

$$\begin{aligned} l &:= \max_k \frac{\sigma_k}{1 + \lambda u^\top S - \lambda u_k S_k} \\ &< \max_k \sigma_k \quad 1 + \lambda u^\top S - \lambda u_k S_k > 1 \\ &= \sigma_{max} \end{aligned}$$

Therefore, l is a reachable point. Moreover, any $\frac{\sigma_{max}}{1 + \lambda u^\top S} < x < l$ will still induce positive y_k for any k and we will also use this to prove that x should not be smaller than l . Let

$$c := \arg \max_k \frac{\sigma_k}{1 + \lambda u^\top S - \lambda u_k S_k}$$

then we can substitute l into the x of y_c . It can be easily verified that $y_c = 1$ at such l . Since y_c is monotonically decreasing in terms of x , any x smaller than l will cause y_c to be greater than 1. At the same time, other y_k is still positive as mentioned just above, so the $\sum_k y_k$ will be greater than 1. Thus, l is a reachable left end point. \square

C. Complete Solutions for M step

$$-\ln \sum_k \sigma_k y_k - \lambda \sum_k u_k S_k \ln y_k. \quad (21)$$

The main case when $u_k S_k > 0$ for all k is presented in the main paper. Here we derive the case when there exist some k such that $u_k S_k = 0$. Assume a non-empty subset of categories/classes

$$K_o := \{k \mid u_k S_k = 0\} \neq \emptyset$$

and its non-empty complement

$$\bar{K}_o := \{k \mid u_k S_k > 0\} \neq \emptyset.$$

In this case the second term (fairness) in our loss (21) does not depend on variables y_k for $k \in K_o$. Also, note that the first term (collision cross-entropy) in (21) depends on these variables only via their linear combination $\sum_{k \in K_o} \sigma_k y_k$. It is easy to see that for any given confidences y_k for $k \in \bar{K}_o$ it is optimal to put all the remaining confidence $1 - \sum_{k \in \bar{K}_o} y_k$ into one class $c \in K_o$ corresponding to the largest prediction among the classes in K_o

$$c := \arg \max_{k \in K_o} \sigma_k$$

so that

$$y_c = 1 - \sum_{k \in \bar{K}_o} y_k \quad \text{and} \quad y_k = 0, \quad \forall k \in K_o \setminus c.$$

Then, our loss function (21) can be written as

$$-\ln \sum_{k \in K_o \cup \{c\}} \sigma_k y_k - \lambda \sum_{k \in K_o} u_k S_k \ln y_k \quad (22)$$

that gives the Lagrangian function incorporating the probability simplex constraint

$$-\ln \sum_{k \in \bar{K}_o \cup \{c\}} \sigma_k y_k - \lambda \sum_{k \in \bar{K}_o} u_k S_k \ln y_k + \gamma \left(\sum_{k \in \bar{K}_o \cup \{c\}} y_k - 1 \right).$$

The stationary point for this Lagrangian function should satisfy equations

$$-\frac{\sigma_k}{\sigma^\top y} - \lambda u_k S_k \frac{1}{y_k} + \gamma = 0, \quad \forall k \in \bar{K}_o \quad \text{and} \quad -\frac{\sigma_c}{\sigma^\top y} + \gamma = 0$$

which could be easily written as a linear system w.r.t variables y_k for $k \in \bar{K}_o \cup \{c\}$.

We derive a closed-form solution for the stationary point as follows. Substituting γ from the right equation into the left equation, we get

$$\frac{\sigma_c - \sigma_k}{\sigma^\top y} y_k = \lambda u_k S_k, \quad \forall k \in \bar{K}_o. \quad (23)$$

Summing over $k \in \bar{K}_o$ we further obtain

$$\frac{\sigma_c(1-y_c) - \sum_{k \in \bar{K}_o} \sigma_k y_k}{\sigma^\top y} = \lambda u^\top S \Rightarrow \frac{\sigma_c - \sigma^\top y}{\sigma^\top y} = \lambda u^\top S$$

giving a closed-form solution for $\sigma^\top y$

$$\sigma^\top y = \frac{\sigma_c}{1 + \lambda u^\top S}.$$

Substituting this back into (23) we get closed-form solutions for y_k

$$y_k = \frac{\lambda u_k S_k}{(1 + \lambda u^\top S)(1 - \frac{\sigma_k}{\sigma_c})}, \quad \forall k \in \bar{K}_o.$$

Note that positivity and boundedness of y_k requires $\sigma_c > \sigma_k$ for all $k \in \bar{K}_o$. In particular, this means $\sigma_c = \sigma_{max}$, but it also requires that all σ_k for $k \in \bar{K}_o$ are strictly smaller than σ_{max} . We can also write the corresponding closed-form solution for y_c

$$y_c = 1 - \sum_{k \in \bar{K}_o} y_k = 1 - \frac{\sigma_c}{1 + \lambda u^\top S} \sum_{k \in \bar{K}_o} \frac{\lambda u_k S_k}{\sigma_c - \sigma_k}.$$

Note that this solution should be positive $y_c > 0$ as well.

In case any of the mentioned constraints ($\sigma_c > \sigma_k, \forall k \in \bar{K}_o$ and $y_c > 0$) is not satisfied, the *complimentary slackness* (KKT) can be used to formally prove that the optimal solution is $y_c = 0$. That is, $y_k = 0$ for all $k \in \bar{K}_o$. This reduces the optimization problem to the earlier case focusing on resolving y_k for $k \in \bar{K}_o$. This case is guaranteed to find a unique solution in the interior of the simplex $\Delta_{\bar{K}_o}$. Indeed, since inequality $u_k S_k > 0$ holds for all $k \in \bar{K}_o$, the strong fairness enforces a log-barrier for all the boundaries of this simplex.

D. Network Architecture

The network structure is VGG-style and adapted from [16].

E. Dataset Summary

Table 8 indicates the number of (training) data and the input size of each image for the unsupervised clustering. Training and test sets are the same.

Grey(28x28x1)	RGB(32x32x3)	RGB(96x96x3)
1xConv(5x5,s=1,p=2)@64	1xConv(5x5,s=1,p=2)@32	1xConv(5x5,s=2,p=2)@128
1xMaxPool(2x2,s=2)	1xMaxPool(2x2,s=2)	1xMaxPool(2x2,s=2)
1xConv(5x5,s=1,p=2)@128	1xConv(5x5,s=1,p=2)@64	1xConv(5x5,s=2,p=2)@256
1xMaxPool(2x2,s=2)	1xMaxPool(2x2,s=2)	1xMaxPool(2x2,s=2)
1xConv(5x5,s=1,p=2)@256	1xConv(5x5,s=1,p=2)@128	1xConv(5x5,s=2,p=2)@512
1xMaxPool(2x2,s=2)	1xMaxPool(2x2,s=2)	1xMaxPool(2x2,s=2)
1xConv(5x5,s=1,p=2)@512	1xConv(5x5,s=1,p=2)@256	1xConv(5x5,s=2,p=2)@1024
1xLinear(512x3x3,K)	1xLinear(256x4x4,K)	1xLinear(1024x1x1,K)

Table 7. Network architecture summary. s: stride; p: padding; K: number of clusters. The first column is used on MNIST [24]; the second one is used on CIFAR10/100 [39]; the third one is used on STL10 [7]. Batch normalization is also applied after each Conv layer. ReLu is adopted for non-linear activation function.

As for **weakly-supervised** classification on STL10, we use 5000 images for training and 8000 images for testing. For CIFAR10, we use 50000 images for training and 10000 images for testing. We only keep a certain percentage of ground-truth labels for each class of training data. The accuracy is calculated on test set by comparing the hard-max of prediction to the ground-truth.

STL10	CIFAR10	CIFAR100-20	MNIST
13000	60000	60000	70000
96x96x3	32x32x3	32x32x3	28x28x1

Table 8. Dataset summary for unsupervised clustering.

F. Experimental Details

Low-level Self-supervised Classification We use one-layer linear classifier for all loss functions except for Kmeans. The weight of the classifier is initialized by using Kaiming initialization [12] and the bias is all set to zero at the beginning. We use the l_2 -norm weight decay and set the coefficient of this term to 0.001, 0.02, 0.009 and 0.02 for MNIST, CIFAR10, CIFAR100 and STL10 respectively. The optimizer is stochastic gradient descent with learning rate set to 0.1 for all. The batch size is set to 250. We set λ in our loss to 100 and use this constant for all experiments.

Deep Self-supervised Classification We use Adam [20] with learning rate $1e^{-4}$ for optimizing the network parameters. We set batch size to 250 for CIFAR10, CIFAR100 and MNIST and we use 160 for STL10. We report the mean accuracy and Std from 6 runs with random initializations. We use 50 epochs for each run and all methods reach convergence within 50 epochs.